

New Coordination Polymer Changing Its Color upon Reversible Deintercalation and Reintercalation of Water: Synthesis, Structure, and Properties of Poly[Diaqua-(μ_2 -Squarato- O,O')-(μ_2 -4,4'-Bipyridine- N,N')-Manganese(II)] Trihydrate

Christian Näther,* Jan Greve, and Inke Jeß

Institut für Anorganische Chemie der Christian-Albrechts-Universität zu Kiel,
Olshausenstrasse 40 (Otto-Hahn-Platz 6-7), D-24098-Kiel, Germany

Received May 23, 2002. Revised Manuscript Received August 19, 2002

The new coordination polymer poly[diaqua-(μ_2 -squarato- O,O')-(μ_2 -4,4'-bipyridine- N,N')-manganese(II)] trihydrate was prepared by hydrothermal reaction of $MnCl_2 \cdot 4 H_2O$ with squaric acid and 4,4'-bipyridine in water. In the crystal structure the manganese atoms are octahedrally coordinated by two squarate anions, two 4,4'-bipyridine ligands, and two water molecules. The squarate anions and the 4,4'-bipyridine ligands connect the metal atoms into interpenetrated sheets and are connected via $O-H \cdots O$ hydrogen bonding. From this arrangement channels are formed in which additional water molecules are intercalated. The channel water molecules can be reversibly de- and intercalated by heating or in a vacuum in a presumably topotactic reaction. The water molecules bound to the manganese atoms can also be removed on heating leading to the new intensely yellow compound $Mn(C_4O_4) \cdot (4,4'-bipyridine)$. Even this compound incorporates water leading to the formation of the starting material. The reaction is accompanied with a change of the color of the material from yellow to colorless. All reactions were investigated using simultaneous differential thermoanalysis, thermogravimetry and mass spectroscopy, ex-situ X-ray powder diffraction and in-situ temperature-resolved X-ray powder diffraction, as well as optical microscopy and UV-vis spectroscopy.

Introduction

The design of new coordination polymers based on transition metal compounds and multidentate organic ligands has attracted much interest in recent years.¹ These compounds are of interest from several points of view. Dependent on the nature of the metal and the coordination behavior of the ligand one can develop synthetic strategies to influence the three-dimensional arrangement in the crystal in a more directed way.¹ Therefore, several such compounds were prepared and structurally characterized during the past few years.^{1,2} One major goal in this area is the preparation of new

compounds with interesting physical properties such as cooperative magnetic phenomena³ or the construction of open framework structures with micropores for ion exchange or catalysis.⁴ In our own investigations we have prepared and characterized several new coordination polymers based on transition metals and multidentate amine ligands such as 4,4'-bipyridine or pyrazine.⁵

* To whom correspondence should be addressed. Fax: +49 (0)431/880-1520. E-mail: cnather@ac.uni-kiel.de.

(1) (a) Hagrman, P. J.; Hagrman, D.; Zubietta, J. *Angew. Chem. 1999*, **111**, 2798; *Angew. Chem., Int. Ed. Engl.* **1999**, **38**, 2638. (b) Batten, S. R.; Robson, R. *Angew. Chem. 1998*, **110**, 1558 and *Angew. Chem., Int. Ed. Engl.* **1998**, **37**, 1460. (c) Robson, R. In *Comprehensive Supramolecular Chemistry*; Pergamon: New York, 1996; Chapter 22, p 733. (d) Moulton, B.; Zaworotko, M. J. *Chem. Soc. Rev.* **2001**, **101**, 1629. (e) Robson, R.; Abrahams, B. F.; Batten, S. R.; Grable, R. W.; Hoskins, B. F.; Liu, J. In *Supramolecular Architecture*. American Chemical Society: Washington, DC, 1992; Chapter 19; (f) Yaghi, O. M.; Li, H.; Davis, C.; Richardson, D.; Groy, T. L. *Acc. Chem. Res.* **1998**, **31**, 474. (g) Batten, S. R. *Curr. Opin. Solid State Mater. Sci.* **2001**, **5**, 107. (h) Batten, S. R. *Cryst. Eng. Commun.* **2001**, **18**. (i) Aakeröy, C. B.; Beatty, A. M. *Aust. J. Chem.* **2001**, **54**, 409. (j) Blake, A. J.; Champness, N. R.; Hubberstey, P.; Li, W.-S.; Schröder, M. *Coord. Chem. Rev.* **1999**, **183**, 17. (k) Holiday, B. J.; Mirkin, C. A. *Angew. Chem. 2001*, **113**, 2076 and *Angew. Chem., Int. Ed.* **2001**, **40**, 2022.

(2) Selected examples are: (a) Riou-Cavallac, M.; Albinet, C.; Gréneche, J.-M.; Férey, G. *J. Mater. Chem.* **2001**, **11**, 3166; (b) Lu, J. Y.; Babb, A. M. *Inorg. Chem.* **2002**, **41**, 1342; (c) Finn, R. C.; Burkholder, E.; Zubietta, J. *Chem. Commun.* **2001**, 1852; (d) Ciurtin, D. M.; Pschirer, N. G.; Smith, M. D.; Bunz, U. H. F.; zur Loye, H.-C. *Chem. Mater.* **2001**, **13**, 2743. (e) Liu, C.-M.; Gao, S.; Hu, H.-M.; Jin, X.; Kou, H.-Z. *J. Chem. Soc., Dalton Trans.* **2002**, 598. (f) Carlucci, L.; Ciani, G.; Proserpio, D. M.; Rizzato, S. *Chem. Eur. J.* **2002**, **8** (7), 1520. (g) Braga, D.; Maini, L.; Polito, M.; Scaccianoce, L.; Cijazzi, G.; Greponi, F. *Coord. Chem. Rev.* **2001**, **216**, 225.

(3) Selected examples are: (a) Sun, H.-L.; Ma, B.-Q.; Gao, S.; Su, G. *Chem. Commun.* **2001**, 2586. (b) Lloret, F.; Julve, M.; Cano, J.; De Munno, G. *Mol. Cryst. Liq. Cryst.* **1999**, **334**, 569. (c) Manson, J. L.; Arif, A. M.; Miller, J. S. *Chem. Commun.* **1999**, 1479. (d) Noro, S.; Kitagawa, S.; Yamashita, M.; Wada, T. *Chem. Commun.* **2002**, 222.

(4) Selected examples are: (a) Reineke, T. M.; Eddaoudi, M.; O'Keeffe, M. O.; Yaghi, O. M. *Angew. Chem.* **1999**, **111**, 2712; *Angew. Chem., Int. Ed.* **1999**, **38**, 2590. (b) Zaworotko, M. J. *Angew. Chem. 2000*, **112**, 3180; *Angew. Chem., Int. Ed.* **2000**, **39**, 3052. (c) Batten, S. R.; Hoskins, B. F.; Robson, R. *Chem. Eur. J.* **2000**, **6** (1), 156.

(5) (a) Näther, C.; Wriedt, C. M.; Jeß, I. *Z. Anorg. Allg. Chem.* **2002**, **628**, 394; (b) Näther, C.; Greve, J.; Jeß, I. *Solid State Sci.* **2002**, **4**, 813. (c) Näther, C.; Jeß, I. *Monatshefte* **2001**, **132**, 897; (d) Näther, C.; Greve, J.; Jeß, I. *Polyhedron* **2001**, **20** (9–10), 1017; (e) Näther, C.; Jeß, I.; Studzinski, H. Z. *Naturforsch.* **2001**, **56b**, 997.

These ligands are excellent for the formation of coordination polymers because they can connect two different metal cations forming linear metal 4,4'-bipyridine or pyrazine chains.⁶ For the connection of the metal cations in such chains we have used small anions which are not conformationally flexible like the squarate anion. For this anion only a limited number of coordination geometries were observed, with most of them leading to linear or corrugated chains.⁷ Therefore, using 4,4'-bipyridine and squarate anions as ligands, two- or three-dimensional structures can be expected which should contain more or less distorted square sheets. Starting from these considerations, we have prepared the new compound poly[diaqua-(μ_2 -squarato-*O,O'*)-(μ_2 -4,4'-bipyridine-*N,N*)-manganese(II)] trihydrate by hydrothermal reaction. In this compound the water molecules can reversibly be removed and intercalated. This process is accompanied with a change of the color of the material as function of water content. In the following we report on these investigations.

Experimental Section

Synthesis of Poly[diaqua-(μ_2 -squarato-*O,O'*)-(μ_2 -4,4'-Bipyridine-*N,N*)-manganese(II)] Trihydrate. The following, in 10 mL of water, were reacted in a Teflon-lined steel autoclave at 150 °C: 99.95 mg (0.5 mmol) MnCl₂·4 H₂O (Merck), 57.48 mg (0.5 mmol) squaric acid (ACROS), and 156.09 mg (1.0 mmol) 4,4'-bipyridine (ACROS). After 7 days the reaction mixture was cooled at a rate of 3 °C/h and the product was filtered off and washed with water. The product consisted of a pure colorless microcrystalline powder of the title compound with crystals too small for single-crystal X-ray analysis. The excess of 4,4'-bipyridine is necessary for the neutralization of the squaric acid. Otherwise, no pure samples could be obtained. Yield: 76.75% (based on MnCl₂·4H₂O). Elemental analysis (%): calculated C, 40.69%; N, 6.78%; H, 4.39%; found C, 40.44%; N, 6.87%; H, 4.51%. X-ray powder diffraction: phase pure.

Single crystals of the compound were prepared using the same reaction conditions, but with only 78.04 mg (0.5 mmol) of 4,4'-bipyridine. In this case, the product contained large colorless crystals of the title compound as the major phase and a small amount of colorless crystals of the manganese squarate dihydrate as the second phase.⁸ The manganese-squarate-tetrahydrate prepared by Weiss et al. did not occur.⁹

X-ray Crystal Structure Determination. The data were measured using an imaging plate diffraction system (IPDS) from STOE & CIE. Structure solution was performed using

(6) Selected examples are: (a) Persky, N. S.; Chow, J. M.; Poschmann, K. A.; Lacuesta, N. N.; Stoll, S. L. *Inorg. Chem.* **2001**, *40*, 29. (b) Moreno, J. M.; Suarez-Varela, J.; Colacio, E.; Avila-Roson, J. C.; Hidalgo, M. A.; Martin-Ramos, D. *Can. J. Chem.* **1995**, *73*, 1591. (c) Kawata, S.; Kitagawa, S.; Kurnagai, H.; Iwabuchi, S.; Katada, M. *Inorg. Chim. Acta* **1998**, *267*, 143. (d) Yaghi, O. M.; Li, G. *Angew. Chem.* **1995**, *107*, 232 and *Angew. Chem., Int. Ed. Engl.* **1995**, *34*, 207. (e) Batten, S. R.; Jeffery, J. C.; Ward, M. D. *Inorg. Chim. Acta* **1999**, *292*, 231. (f) Jack, Y. L.; Cabrera, B. R.; Wang, R.-J.; Li, J. *Inorg. Chem.* **1999**, *38*, 4608. (g) Graham, P. M.; Pike, R. D.; Sabat M.; Bailey, R. D.; Pennington, W. T. *Inorg. Chem.* **2000**, *39*, 5121. (h) Masciocchi, N.; Cairati, P.; Carlucci, L.; Mezza, G.; Ciani, G.; Sironi, A. *J. Chem. Soc., Dalton Trans.* **1996**, 2739.

(7) Selected examples are: (a) Alleyne, B. D.; Hall, L. A.; Hosein, H.-A.; Jaggernauth, H.; White, A. J. P.; Williams, D. J. *J. Chem. Soc., Dalton Trans.* **1998**, 3845. (b) Zheng, L.-M.; Fang, X.; Lii, K.-H.; Song, H.-H.; Xin, X.-Q.; Fun, H.-K.; Chinnakali, K.; Abdul Razak, I. *J. Chem. Soc., Dalton Trans.* **1999**, 2311. (c) Huang, S. D.; Shan, Y. *J. Solid State Chem.* **2000**, *152*, 229. (d) Yufit, D. S.; Price, D. J.; Howard, J. A. K.; Gutschke, S. O. H.; Powell, A. K.; Wood, P. T. *Chem. Commun.* **1999**, 1561.

(8) Greve, J. Diploma Thesis, 2000, University of Kiel.

(9) Weiss, A.; Riegler, E.; Alt, I.; Böhme, H.; Robl, Ch. *Z. Naturforsch.* **1996**, *41b*, 18.

Table 1. Crystal Data and Results of the Structure Refinement for Poly[Diaqua-(μ_2 -squarato-*O,O'*)-(μ_2 -4,4'-bipyridine-*N,N*)-manganese(II)] Trihydrate

formula	[Mn(C ₄ O ₄)(C ₁₀ H ₈ N ₂)(H ₂ O) ₂]·3H ₂ O
MW (g·mol ⁻¹)	413.24
crystal color	colorless
crystal system	monoclinic
space group	<i>P</i> 2 ₁ / <i>c</i>
<i>a</i> (Å)	18.716 (1)
<i>b</i> (Å)	11.544 (1)
<i>c</i> (Å)	8.1738 (5)
β (°)	90.536 (7)
<i>V</i> (Å ³)	1766.0 (2)
temperature (K)	130
<i>Z</i>	4
<i>D</i> _{calcd.} (g·cm ⁻³)	1.554
<i>F</i> (000)	852
2θ range	3–56°
<i>h/k/l</i> ranges	24/-24, -15/15, -10/10
μ (Mo $\text{K}\alpha$)/mm ⁻¹	0.80
measured refl.	15125
<i>R</i> _{int.}	0.0343
independent refl.	4026
refl. with <i>I</i> > 2σ(<i>I</i>)	3254
refined parameters	278
<i>R</i> ₁ [<i>I</i> > 2σ(<i>I</i>)]	0.0342
w <i>R</i> ₂ [all data]	0.0919
<i>GOF</i>	1.027
Min./max. res. (e·Å ⁻³)	0.32/-0.31

SHELXS-97¹⁰ and structure refinement was done against *F*² using SHELXL-97.¹¹ All non-hydrogen atoms were refined using anisotropic displacement parameters. The C–H hydrogen atoms were positioned with idealized geometry and refined with isotropic displacement parameters using the riding model, whereas the O–H hydrogen atoms were located from difference map and were refined with varying coordinates and varying isotropic displacement parameters. Selected crystal data and results of the structure refinement are given in Table 1.

Crystallographic data have been deposited with the Cambridge Crystallographic Data Centre (CCDC 191338). Copies may be obtained free of charge on application to the Director, CCDC, 12 Union Road, Cambridge CB2 1E2, UK (fax, int.code +44)01223/3 36-033; or e-mail, deposit@chemcrys.cam.ac.uk).

X-ray Powder Diffraction Experiments. X-ray powder diffraction experiments were performed using a STOE STADI P transmission powder diffractometer with a 4° position sensitive detector (PSD) using Cu $\text{K}\alpha$ -radiation (λ = 1.540598 Å). For temperature- or time-dependent X-ray powder diffraction experiments the diffractometer is equipped with a graphite oven and a position-sensitive detector (scan range 5–50°) from STOE & CIE. All temperature- and time-resolved X-ray powder experiments were performed in glass capillaries under a static air atmosphere.

Differential Thermal Analysis, Thermogravimetry, and Mass Spectroscopy. DTA-TG measurements were performed in Al₂O₃ crucibles using simultaneously a STA-429 balance from Netzsch with different heating rates under a dynamic argon (purity 4.6) and air atmosphere (flow rate 100 mL/min). DTA-TG-MS measurements were performed simultaneously using the STA-409CD with Skimmer coupling from Netzsch, which was equipped with a quadrupol mass spectrometer QMA 400 (max. 512 amu) from Balzers. The MS measurements were performed in analogue and trend scan mode. The investigations were performed in Al₂O₃ crucibles under a dynamic helium atmosphere (flow rate 75 mL/min, purity 4.6) using a heating rate of 4 K/min. All measurements were corrected for buoyancy and current effects.

(10) Sheldrick, G. M. SHELXS-97, Program for Crystal Structure Solution; University of Göttingen, Germany, 1997.

(11) Sheldrick, G. M. SHELXL-97, Program for the Refinement of Crystal Structural Data; University of Göttingen, Germany, 1997.

Optical Microscopy. Optical microscopy was performed using Olympus BX and SZX12 microscopes, which are equipped with a video camera. The investigations were performed in glassy crucibles under a humid air atmosphere.

UV-Vis Measurements: UV-vis spectra were collected using a Varian Cary 5 UV-vis spectrometer. The measurements were carried out in reflection geometry using an "Ulbricht-Kugel" and BaSO_4 as the standard. The reflectance spectra were corrected against the BaSO_4 standard and converted into absorption spectra using the Kubelka-Munk function.¹² A freshly prepared sample was evacuated until all the channel water molecules were removed, stored on air for some time, and then measured again. The measurements were repeated until no change of the actual spectra was observed.

Elemental Analysis. C, H, N analysis was performed using a Heraeus CHN-O-RAPID combustion analyzer. Elemental analysis of a sample in which the water molecules were completely removed by heating was as follows: calculated C, 52.03%; N, 8.67%; H, 2.50%; found C, 51.84%; N, 8.45%; H, 2.60%.

Results and Discussion

Crystal Structures. The title compound poly[di-aqua- $(\mu_2\text{-squarato-}O,O')\text{-4,4'}\text{-bipyridine-manganese(II)}$] trihydrate crystallizes in the centrosymmetric space group $P2_1/c$ with four formula units in the unit cell. The asymmetric unit contains two crystallographically independent Mn^{2+} cations and squarate dianions, each of them located on a center of inversion, as well as one 4,4'-bipyridine ligand and five water molecules in general positions. The metal cations are coordinated by two squarate dianions, two 4,4'-bipyridine ligands, and two water molecules to form a distorted octahedron (Figure 1). Bond lengths and angles are comparable to those of related structures retrieved from the Cambridge Structural Database¹³ (Table 2).

The Mn^{2+} cations are connected by the squarate dianions via $\mu\text{-}O,O'$ coordination forming "zigzag"-chains into the direction of the crystallographic *c*-axis (Figure 1). In the coordination of each metal cation only one squarate oxygen atom is involved. Obviously, the direct coordination in which two squarate oxygen atoms are involved is less favorable. The C–O–Mn angles amount to 130.8 and 132.7° and the cations deviate 0.409 and 0.705 Å from the plane formed by the four-membered squarate ring. This demonstrates that the cations are rather oriented into the direction of one of the lone pair of the squarate ligand.

The Mn^{2+} cations in these chains are connected by the 4,4'-bipyridine ligands forming sheets parallel to (010), which contain pores of about 7.5×11 Å. The cations are located in the plane of the six-membered 4,4'-bipyridine ring and the angles C–N–Mn amount to 119.3 and 121.3°. The sheets are stacked perpendicular to the *c*-axis (Figure 2) and interpenetrate with symmetry equivalent sheets generated by the 2_1 -axis forming a three-dimensional arrangement. The connection of the interpenetrating networks is achieved via O–H···O hydrogen bonding between the hydrogen atoms of the water molecules bound to the metal cations and the oxygen atoms of the squarate dianions, which

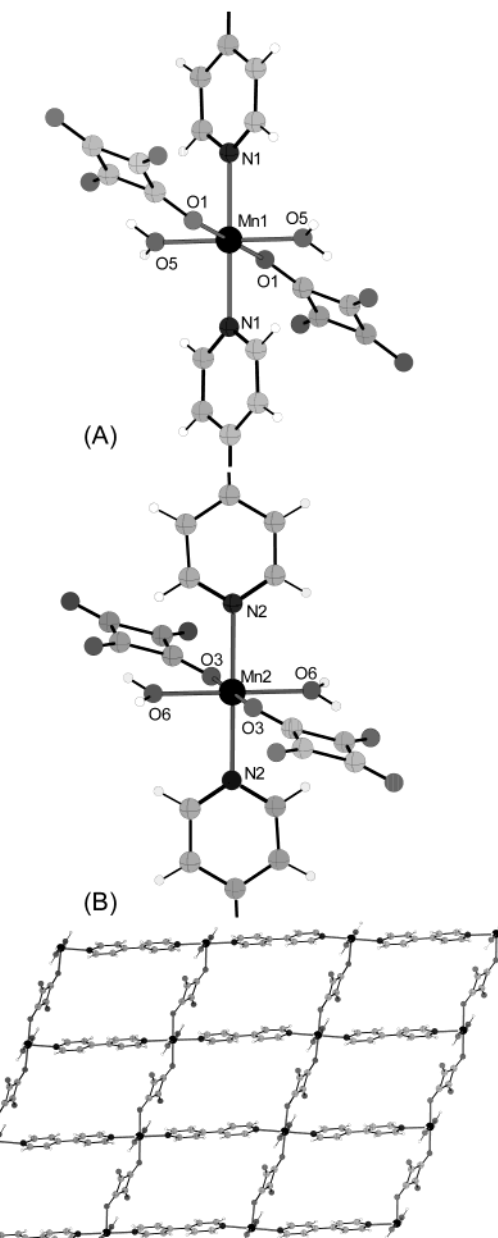


Figure 1. Crystal structure of poly[diaqua- $(\mu_2\text{-squarato-}O,O')\text{-}(\mu_2\text{-4,4'}\text{-bipyridine-}N,N)\text{-manganese(II)}$] trihydrate with view of the Mn coordination with labeling (A) and with view on the 2-dimensional network (B) (In Figure 1A only half of the 4,4'-bipyridine ligand is presented).

are not involved in Mn coordination. The intermolecular O···H distances of 1.85 and 1.87 Å, the O···O distances of 2.69 and 2.72 Å, and the O–H···O angles of 160 and 163° show that these are strong hydrogen bonds. From this arrangement channels are formed parallel to the crystallographic *c*-axis which host three water molecules per formula unit in an ordered manner. These water molecules are only weakly bound and can be removed very easily in a vacuum or by heating (see below).

Thermoanalytical Investigations. On heating a sample of the title compound, and using simultaneously differential thermoanalysis (DTA), thermogravimetry (TG), and mass spectroscopy (MS), two endothermic events are observed at peak temperatures of 76 and 128 °C which are accompanied with two mass steps of about 11.7 and 8.5% in the TG curve (Figure 3).

(12) Kortüm, G. *Reflectance Spectroscopy*; Springer-Verlag: New York, 1969.

(13) (a) Cambridge Structural Database 2001, Version 1.2. (b) Allen, F.; Kennard, O. *Chem. Des. Autom. News* **1993**, 8 (1), 31.

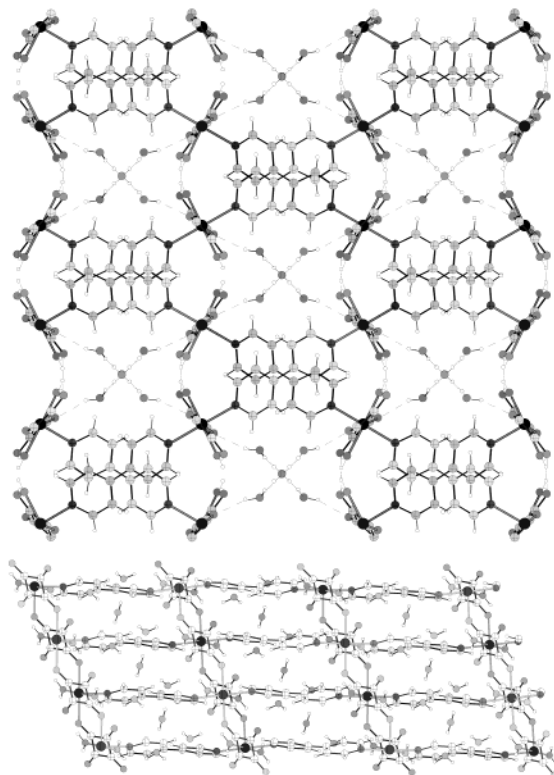


Figure 2. Crystal structure of poly[diaqua-(μ_2 -squarato- O,O')-(μ_2 -4,4'-bipyridine- N,N')-manganese(II)] trihydrate with view along the c -axis (top) and along the b -axis (bottom). Hydrogen bonding is shown as dotted lines.

Table 2. Selected Bond Lengths (Å) and Angles (°) for Poly[diaqua-(μ_2 -squarato- O,O')-(μ_2 -4,4'-bipyridine- N,N')-manganese(II)] Trihydrate

Mn(1)	–	O(5)	2.160	(2)	($\times 2$)		
Mn(1)	–	O(1)	2.190	(1)	($\times 2$)		
Mn(1)	–	N(1)	2.290	(2)	($\times 2$)		
Mn(2)	–	O(6)	2.146	(2)	($\times 2$)		
Mn(2)	–	O(3)	2.159	(2)	($\times 2$)		
Mn(2)	–	N(2)	2.320	(2)	($\times 2$)		
O(5)	–	Mn(1)	–	O(1)	92.07	(4)	($\times 2$)
O(5)	–	Mn(1)	–	O(1)	87.93	(4)	($\times 2$)
O(5)	–	Mn(1)	–	N(1)	93.02	(4)	($\times 2$)
O(1)	–	Mn(1)	–	N(1)	94.93	(4)	($\times 2$)
O(5)	–	Mn(1)	–	N(1)	86.98	(4)	($\times 2$)
O(1)	–	Mn(1)	–	N(1)	85.07	(4)	($\times 2$)
O(5)	–	Mn(1)	–	O(5)	180.0		
O(1)	–	Mn(1)	–	O(1)	180.0		
N(1)	–	Mn(1)	–	N(1)	180.0		
O(6)	–	Mn(2)	–	O(3)	93.05	(4)	($\times 2$)
O(6)	–	Mn(2)	–	O(3)	86.95	(4)	($\times 2$)
O(6)	–	Mn(2)	–	N(2)	90.86	(4)	($\times 2$)
O(6)	–	Mn(2)	–	N(2)	89.14	(4)	($\times 2$)
O(3)	–	Mn(2)	–	N(2)	93.73	(4)	($\times 2$)
O(3)	–	Mn(2)	–	N(2)	86.27	(4)	($\times 2$)
O(6)	–	Mn(2)	–	O(6)	180.0		
O(3)	–	Mn(2)	–	O(3)	180.0		
N(2)	–	Mn(2)	–	N(2)	180.0		

According to the MS measurements, in this step only water ($m/z = 18$) is emitted. From the mass loss and structural considerations it can be assumed that the first signal corresponds to the removal of the channel water molecules and the second signal corresponds to the loss of those water molecules that are coordinated to the metal cations.

The observed values are somewhat lower than those calculated ($\Delta m_{\text{theo}}: -3 \text{ H}_2\text{O} = -13.08\%$; $-2 \text{ H}_2\text{O} = -8.72\%$). However, in several DTA-TG experiments

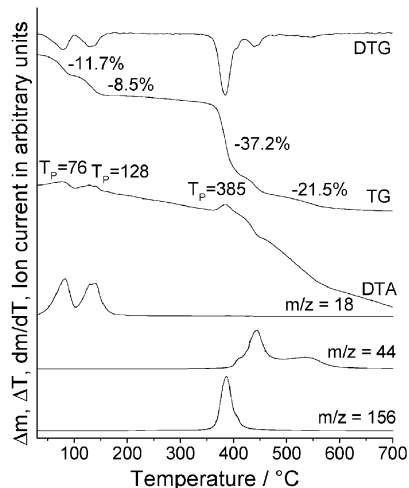


Figure 3. DTA, TG, DTG, and MS trend scan curves for poly[diaqua-(μ_2 -squarato- O,O')-(μ_2 -4,4'-bipyridine- N,N')-manganese(II)] trihydrate (simultaneous measurement; powdered crystals; weight 13.95 mg; heating rate 4 °C/min.; dynamic helium atmosphere; flow rate 75 mL/min.; $m/z = 18$, water; $m/z = 44$, CO_2 (squareate); $m/z = 156$, 4,4'-bipyridine; Al_2O_3 -crucible; the mass changes are given in % and the peak temperatures T_p are given in °C).

these values always differ slightly, which can be regarded either to the preparation of the material or to a precedent partial loss of the water molecules dependent on the history of the samples. On further heating the sample decomposes in two steps which can be clearly seen from the DTG curve. The MS measurements show that at first the 4,4'-bipyridine ligand is emitted ($m/z = 156$) and finally the squareate anions decompose. However, these two steps cannot be resolved successfully. The experimental mass loss is in good agreement with that calculated. In the final product of this reaction only MnO could be detected by X-ray powder diffraction. When the sample was heated in air, similar observations were made. In this case, the decomposition of the pure Mn-squareate-4,4'-bipyridine intermediate starts at lower temperatures and proceeds via an exothermic reaction. The final product in this reaction consists of Mn_2O_3 .

Investigations on the Mechanism and the Reversibility of the Removal of the Water Molecules. A part of the water molecules can also be removed by applying a vacuum. To investigate the reversibility of this reaction, additional experiments with thermogravimetry using isothermal conditions and ex-situ and in-situ temperature-resolved X-ray powder diffraction were performed. When the water is removed by applying vacuum a mass loss of about 12.8% is measured, which is in good agreement with the removal of three water molecules ($\Delta m_{\text{theo}}: -3 \text{ H}_2\text{O} = -13.08\%$). Because only three equiv of water can be removed by evacuation, one can assume that only the channel water molecules are emitted. If also some coordinated water molecules were to be removed the reaction could not be stopped at this point on further evacuation. However, if at this point the sample was subjected to a humid gas flow in a thermobalance for several days, an increase of the sample mass would be observed, reaching a value which corresponds nearly to the intercalation of three equivs of water. The increase of the sample mass is large at the beginning of the reaction and slows down with

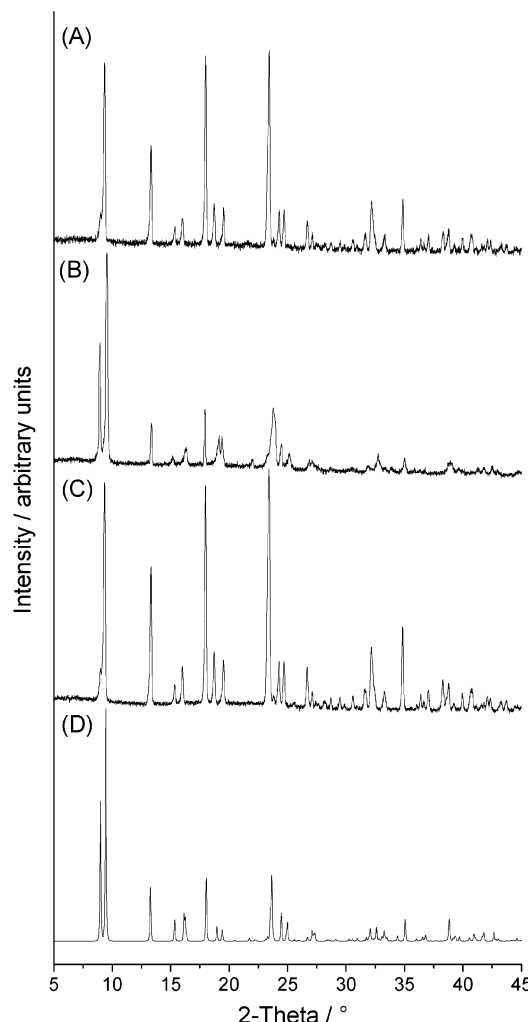


Figure 4. Ex-situ time-resolved powder patterns for poly[diaqua-(μ_2 -squarato- O,O')-(μ_2 -4,4'-bipyridine- N,N')-manganese(II)] trihydrate: powder pattern of a freshly prepared sample (A); after removal of the three water molecules (B); and after storage for 2 d in a humid atmosphere (C); as well as calculated powder pattern for the dehydrated compound poly[diaqua-(μ_2 -squarato- O,O')-(μ_2 -4,4'-bipyridine- N,N')-manganese(II)] (D); (CuK α radiation; transmission geometry; glass capillary; powdered single crystals; the pattern of the dehydrated sample was calculated using the data from the original trihydrate without consideration of the three channel water molecules).

increasing reaction time, which is expected if the reaction is controlled by diffusion within the channels. However, the removal of the channel water molecules seems to be fully reversible. This is evidenced by ex-situ time-resolved X-ray powder diffraction experiments shown in Figure 4. When a freshly prepared sample of the title compound is evacuated until the incorporated channel water is removed, only slight changes in the powder pattern are observed. Some of the reflection positions are shifted, which can be attributed in part to an anisotropic change of the lattice parameters. When the sample is afterward suspended to a saturated water atmosphere for some time the powder pattern is comparable to that of the starting phase. The observed changes in the powder pattern are in agreement with observations made on single-crystal investigations.

In these experiments two complete data sets were measured for one single crystal using an area detector. The first data set was collected for a freshly prepared

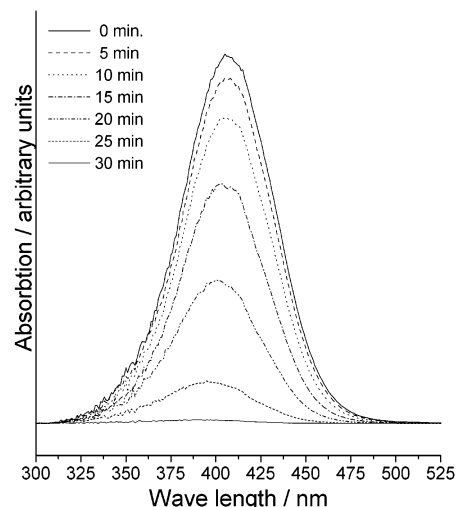


Figure 5. Change of the intensity of the absorption band in the visible range when a sample in which the channel water molecules were removed in a vacuum is stored on air.

crystal and the second one was prepared after this crystal had been evacuated for several hours. The overall diffraction pattern before and after evacuation is comparable and only a broadening of most of the reflections is observed. Indexing the reflections yields the same monoclinic metric, and refinement of the lattice parameters show only a small decrease of the unit cell volume. However, the quality of the second data set measured was extremely poor and the structure refinement does not allow a definite determination of the water content. Nevertheless, these investigations demonstrate that the removal of the channel water molecules should be topotactic.

The intercalation or deintercalation of the channel water molecules is accompanied by significant changes of the color and therefore can be followed by optical microscopy. When a freshly prepared sample of the title compound is evacuated for several hours the color changes from colorless to light yellow. When the sample is then stored in a saturated water atmosphere a continuous change in the color of the starting material is observed. This process can also be followed using ex-situ time-resolved UV-vis measurements of deintercalated samples. A continuous decrease of the absorption band in the visible range is found during the intercalation of water (Figure 5).

If the water is removed completely in a TG experiment the residue is intensively yellow colored and its diffraction pattern is completely different from that of the starting material (Figures 6 and 7). Elemental analysis of this residue is in good agreement with that calculated (see Experimental Section). However, if the residue is stored during the night in a saturated water atmosphere the original color disappears and the diffraction pattern of this sample is identical with that calculated for the starting compound (Figures 6 and 7). Therefore, even this reaction seems to be fully reversible.

Removal of the water molecules can also be followed by in-situ temperature resolved X-ray powder diffraction (Figure 8). Starting at about 110 °C, slight changes of the diffraction pattern are observed which correspond to the removal of the channel water molecules. On

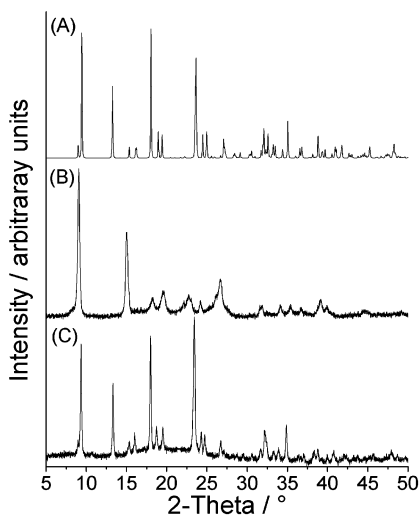


Figure 6. Calculated X-ray powder pattern for poly[diaqua- $(\mu_2\text{-squarato-}O,O')\text{-}(\mu_2\text{-4,4'}\text{-bipyridine-}N,N)$]-manganese(II)] trihydrate (A), experimental powder pattern after the water is completely removed (B), and experimental pattern after the dehydrated sample is stored in a saturated water atmosphere for 12 h (C).

further heating a second transition is observed which is accompanied with larger changes of the pattern due to the removal of the water molecules coordinated to the metal atom. The reason that all transition temperatures are shifted to higher values compared to those measured in the DTA-TG-MS experiments is due to the different experimental conditions. In the X-ray powder measurements the reaction is performed in thin glass capillaries and a static air atmosphere which means that the emitted water molecules are only slowly transported out of the capillary. Therefore, the reaction took place partly under a self-produced atmosphere which is enriched with water.

Conclusions

In the present work we have shown that starting from simple geometrical considerations which are based on the coordination behavior of organic ligands, the structure of coordination polymers can be influenced in a more directed way. However, the actual three-dimensional arrangement is difficult to predict because for the

interaction of the Mn squareate 4,4'-bipyridine sheets observed in the present compound several possibilities, such as stacking or interpenetrating, must be considered. For the directed design of structures with larger pores one has to solve the problem of interpenetrating, which is frequently observed in the structures of such coordination polymers. The occurrence of channels in the present compound formed by the interpenetrating sheets is accidental and their formation and size cannot be planned at all. However, the structure of the present compound stabilized by metal coordination and hydrogen bonding is obviously flexible and stable enough so that the channel water molecules can be reversibly deintercalated and reintercalated. The structures of the intercalated and the deintercalated material are strongly related and both processes seems to be proceed via a topotactic reaction. If the water is completely removed, which means that the water coordinated to the metal centers is also removed, the residue is intensively yellow and the starting material is retained when stored in a saturated water atmosphere. Concerning the mechanism of this step, the X-ray diffraction experiments gave no hint that this reaction is also topotactic. Nevertheless, it is highly likely that the structure of the water-free compound is related to that of the starting material, because the networks are interpenetrated and therefore locked, even without hydrogen bonding of the coordinated water molecules. After the removal of the coordinated water molecules the manganese atoms would be only four-coordinated which is unlikely, even if a tetrahedral coordination for manganese is known.¹⁴ Therefore, it can be assumed that each oxygen atom from the squarate anions which is not involved in metal coordination will coordinate to the manganese atoms under reformation of the octahedral coordination. This would be an explanation for the observed color changes upon the removal of the water molecules, because stronger interactions between the manganese atoms and the squarate anions can be expected. Therefore, the elucidation of the exact mechanism will be the subject of further investigations using magnetic measurements and spectroscopic investigations. These will also include structural investigations of the water-free manganese-squarate(4,4'-bipyridine) compound. However, it is well-known that porous materials change their colors when different solvents are intercalated.¹⁵ Therefore, we will



Figure 7. View of a sample of poly[diaqua- $(\mu_2\text{-squarato-}O,O')\text{-}(\mu_2\text{-4,4'}\text{-bipyridine-}N,N)$]-manganese(II)] trihydrate in which the water was completely removed (left) and after it was stored in a saturated air atmosphere (right).

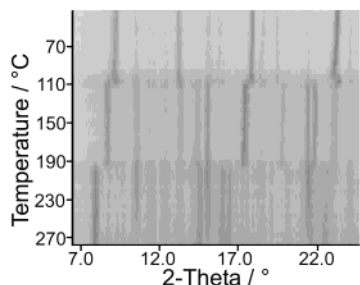


Figure 8. Results of the in-situ temperature-resolved X-ray powder investigations on poly[diaqua- $(\mu_2$ -squarato- O,O')- $(\mu_2$ -4,4'-bipyridine- N,N')-manganese(II)] trihydrate (static air atmosphere; glass capillaries; heating rate 2 °C/min; powder pattern measured every 5 °C).

investigate whether other small molecules can be intercalated in the title compound.

Acknowledgment. We gratefully acknowledge the financial support by the State of Schleswig-Holstein. We are very thankful to Professor Dr. Wolfgang Bensch for helpful discussions, financial support, and the facility to use his experimental equipment.

Supporting Information Available: Tables of X-ray crystallographic data, atomic coordinates and displacement parameters, and bond lengths and angles; and figures of color change of compound studied (PDF). An electronic X-ray crystallographic data file (CIF). This material is available free of charge via the Internet at <http://pubs.acs.org>.

CM021212T

(14) Seipp, E.; Hoppe, R. *Z. Anorg. Allg. Chem.* **1985**, *530*, 117.
 (15) Blanford, C. F.; Schröden, R. C.; Al-Daous, M.; Stein, A. *Adv. Mater.* **2001**, *13*, 26 and literature cited therein.